NASA/TM–2014-218551

Delay of Transition Using Forced Damping

Reginald J. Exton
Langley Research Center, Hampton, Virginia

November 2014

NASA STI Program . . . in Profile

Since its founding, NASA has been dedicated to the advancement of aeronautics and space science. The NASA scientific and technical information (STI) program plays a key part in helping NASA maintain this important role.

The NASA STI program operates under the auspices of the Agency Chief Information Officer. It collects, organizes, provides for archiving, and disseminates NASA's STI. The NASA STI program provides access to the NASA Aeronautics and Space Database and its public interface, the NASA Technical Report Server, thus providing one of the largest collections of aeronautical and space science STI in the world. Results are published in both non-NASA channels and by NASA in the NASA STI Report Series, which includes the following report types:

- TECHNICAL PUBLICATION. Reports of completed research or a major significant phase of research that present the results of NASA Programs and include extensive data or theoretical analysis. Includes compilations of significant scientific and technical data and information deemed to be of continuing reference value. NASA counterpart of peer-reviewed formal professional papers, but having less stringent limitations on manuscript length and extent of graphic presentations.

- TECHNICAL MEMORANDUM. Scientific and technical findings that are preliminary or of specialized interest, e.g., quick release reports, working papers, and bibliographies that contain minimal annotation. Does not contain extensive analysis.

- CONTRACTOR REPORT. Scientific and technical findings by NASA-sponsored contractors and grantees.

- CONFERENCE PUBLICATION. Collected papers from scientific and technical conferences, symposia, seminars, or other meetings sponsored or co-sponsored by NASA.

- SPECIAL PUBLICATION. Scientific, technical, or historical information from NASA programs, projects, and missions, often concerned with subjects having substantial public interest.

- TECHNICAL TRANSLATION. English-language translations of foreign scientific and technical material pertinent to NASA's mission.

Specialized services also include organizing and publishing research results, distributing specialized research announcements and feeds, providing information desk and personal search support, and enabling data exchange services.

For more information about the NASA STI program, see the following:

- Access the NASA STI program home page at *http://www.sti.nasa.gov*

- E-mail your question to help@sti.nasa.gov

- Fax your question to the NASA STI Information Desk at 443-757-5803

- Phone the NASA STI Information Desk at 443-757-5802

- Write to:
  STI Information Desk
  NASA Center for AeroSpace Information
  7115 Standard Drive
  Hanover, MD 21076-1320

NASA/TM–2014-218551

Delay of Transition Using Forced Damping

Reginald J. Exton
Langley Research Center, Hampton, Virginia

National Aeronautics and
Space Administration

Langley Research Center
Hampton, Virginia 23681-2199

November 2014

Available from:

NASA Center for AeroSpace Information
7115 Standard Drive
Hanover, MD 21076-1320
443-757-5802

Delay of Transition Using Forced Damping

Reginald J. Exton
Advanced Measurements and Data Systems Branch
Research Directorate
N.A.S.A. Langley Research Center
Hampton, Virginia 23681-2199

Abstract:

Several experiments which have reported a delay of transition are analyzed in terms of the frequencies of the induced disturbances generated by different flow control elements. Two of the experiments employed passive stabilizers in the boundary layer, one leading-edge bluntness, and one employed an active spark discharge in the boundary layer. It is found that the frequencies generated by the various elements lie in the damping region of the associated stability curve. It is concluded that the creation of strong disturbances in the damping region stabilizes the boundary-layer and delays the transition from laminar to turbulent flow.

Symbols:

S_t Strouhal number
St Stanton number
U velocity (in the boundary-layer) at the effective diameter of an isolated trip
u velocity (in the boundary-layer) at the top of a corrugation
s distance between corrugation peaks
α_i imaginary part of the disturbance wave number
α_r real part of the disturbance wave number
b bluntness of leading-edge
d effective diameter of isolated trip
δ boundary-layer thickness
δ^* boundary-layer displacement thickness
M Mach number
R_o Free-Stream Unit Reynolds number
R_c Cone Transition Reynolds number
R_p Planar Transition Reynolds number
R_{δ^*} Reynolds number based on boundary-layer displacement thickness
k trip height
f dimensional frequency
f_c corrugation frequency
f_{vs} vortex shedding frequency
F dimensionless frequency parameter

Introduction:

The design of aircraft is highly dependent on the dynamics of the fluid flow around the craft. For 100 years, it has been recognized that the flow in a thin boundary layer on the surface is critical to the efficient design of the aircraft. The flow in the boundary layer is initially laminar, but at some point transitions to a turbulent flow increasing the drag (and heat transfer) on the vehicle. As a result, research on methods to reduce the skin friction drag through laminar flow control is a major objective of aerodynamic research. The amplification of instabilities in the boundary layer is thought to be the dominant effect leading to turbulence. The instabilities may be generated directly from elements within the boundary layer or imposed from external sources and usually result in an advance of transition. An early review of the receptivity of the boundary layer to various on-board as well as off-board disturbances is outlined by Reshotko[1]. A more recent review of stability and transition in boundary layers is given by Saric et al. [2].

Occasionally, experiments report a delay of transition as a result of surface modifications. The objective of this paper is to analyze several of these experiments in terms of the frequency of the induced disturbances brought about by these modifications. The disturbances are generated in the boundary layer by several different methods. The frequencies of the various induced disturbances are calculated to be in the damping region of the associated stability curve. This results in stabilization of the boundary layer and to a delay of the transition from laminar to turbulent flow.

Boundary-Layer Flow Control Mechanisms:

Decades of research in aerodynamics have shown little progress in delaying transition. Many attempts to modify the boundary-layer flow have been tried, but most lead to an advance of transition. Some small encouraging success has been observed, but it has been difficult to identify the critical elements of the process in order to be able to develop a given technique to a practical level. A few of the techniques investigated thus far are listed below:

1) Distributed Roughness: Early attempts included very thin modifications of the surface such as the addition of sandpaper, scotch tape, or flapping layers.
2) Riblets: These are long grooves machined into the surface and aligned along the stream-wise direction of the flow. Walsh [3].
3) Blowing/Suction: Although structurally demanding, this technique has been employed to an advantage in special locations.
4) Cooling: Cooling of the surface appears to exhibit an advantage in delaying transition, but has not been demonstrated to be a practical method. Potter [4].
5) Isolated Roughness Elements (Trips): Physical trips have been tried in a variety of shapes, sizes, and configurations with some success. In most of the experiments, the height of the trip, k, is a small fraction of the boundary-layer thickness, $\{k / \delta << 1\}$. Saric et al. [5].

6) Bluntness: Leading-edge bluntness on slender models can often bring about a delay in transition, but is not a practical solution for shaped wings. Brinich and Sands [6], Potter and Whitfield [7].
7) DBD's (Dielectric Barrier Discharges): These surface plasma discharges have been shown to successfully modify flow, but on a very small scale. The small scale is a result of the weak momentum transfer from the plasma to the flow, making it difficult to envision their use in a full scale environment. T. C. Corke et al. [8].
8) Forced Streaks: Delay of transition has been observed in the presence of streamwise forced streaks at low velocities (5 m/sec). The delay has been ascribed to the stabilizing action of the streaks on low amplitude TS waves in the boundary layer. J. H. M. Fransson et al. [9].

Stability Theory and Transition:

A stability theory has been developed by Mack [10] to calculate the conditions for a boundary-layer to transition from laminar to turbulent flow. The theory is based on individual oscillatory vorticity waves, (the Tollmien-Schlichting, or TS, waves), and calculates for a given wave frequency and Reynolds number, where the wave will be damped, neutral, or amplified. The amplitude of the waves is assumed to be weak initially so that a linear theory can be used. Ultimately, when the wave amplitude becomes large enough, nonlinear processes take over, triggering the laminar to turbulent transition. The theory is developed using a series expansion which leads to an infinite sequence of terms which are denoted modes. Mode 1 describes the TS waves just mentioned. Mode 2 exhibits order of magnitude higher frequencies than mode 1, and experiments have shown them to be in resonance with the boundary layer (i.e. $\lambda \approx 2\,\delta$), identifying them as an acoustical mode. Mode 2 has been observed mainly in blowdown facilities in which high pressure air is forced thru a small nozzle in order to generate high velocities. This process generates high frequency sound waves, which are then captured in the boundary-layer of the tunnel walls, before impinging on the model itself. Many attempts have been made to reduce this effect, resulting in "quiet" tunnels.

Arnal [11] has computed detailed stability diagrams for two-dimensional waves (adiabatic wall) for Mach numbers 0, 1.3, 2.2, 3, 4.5, 4.8, 5.8, 7, and 10. Cebeci and Cousteix [12] show additional results obtained by Arnal for Mach numbers 0.6, 0.9, and 1.1. For stability diagrams up to Mach 3.0, only mode 1 instabilities are indicated, while above Mach 3, the higher frequency mode 2 appears and begins to be blended with mode 1. An example of a stability diagram is shown in figure 1 as computed by Arnal [11] for an adiabatic, flat-plate (planar) geometry at Mach 2.2. It shows the range of instabilities versus the Reynolds number, R_{δ^*}. It must be recognized that the stability diagrams as calculated are for ideal flat-plate conditions, and can change for other configurations and practical applications.

A vertical cut thru figure 1 at $R_{\delta^*} = 3 \times 10^3$ is shown in figure 2 which displays the amplification rate as a function of the dimensional frequency for this particular Reynolds number. Experimental measurements have verified this general form in the amplification region (above zero). The dotted segments are extrapolations into the damping region (below zero). Very few experimental rate measurements have been made in the damping region. Between the frequencies A and B, fluctuations are amplified (an unstable flow), ultimately resulting in the transition of laminar to turbulent flow. Fluctuations exhibiting frequencies lower than A, or above B, are expected to be damped and to stabilize the flow.

Induced Disturbances and Delay of Transition:

The following experimental observations of the delay of transition result from the generation of strong disturbances in the flow at specific frequencies (repetition rates). These frequencies lie in the damping region of the associated amplification rate curve. With the exception of the leading-edge bluntness experiment, the disturbances are generated in the boundary-layer thru passive or active stabilizers on the surface of the model. The passive stabilizers generate the specific frequency by having a particular geometry and dimensions. They exhibit a significant height, k, but less than the boundary layer thickness, {$k / \delta < 1$}. The active stabilizers are spark discharges that are initiated on the surface of a flat-plate model.

1) Passive Spherical Trips

Holloway and Sterrett [13] employed a single row of spherical trips of various sizes on a flat-plate model to study boundary-layer transition and heat transfer at Mach numbers of 4.8 and 6.0. Heat transfer was determined by a line of thermocouples aligned along the model length. Spheres with a trip height, k, larger than the boundary-layer thickness, δ, generated an advance of transition; whereas spheres with a trip height smaller than δ led to a delay of transition. Figure 3 {figure 6(a) in Holloway and Sterrett} shows heating rates at Mach 6 for two of the sizes, $k/\delta = 1.85$, and $k/\delta = 0.76$, to illustrate the effect. The no trip condition is designated as $k/\delta = 0$. Figure 4 shows the size and height of the spherical trips described in figure 3 relative to the boundary-layer thickness, δ. The larger trip, with $k/\delta = 1.85$, protrudes through the boundary layer generating turbulence and advancing transition. The smaller trip, with $k/\delta = 0.76$, is embedded in the boundary layer and involves more subtle effects. The vortex shedding frequency, f_{vs}, of this trip is given by,

$$f_{vs} = S_t \, [U / d] \qquad (1)$$

where S_t is the Strouhal number, d is the effective diameter of the truncated sphere, and U is the velocity in the boundary-layer at the height of the effective diameter. The smaller trip is a truncated sphere with an effective diameter, d, of 0.00256 ft 0.78 mm), at a point in the boundary layer where the velocity, U, is 704 ft/sec 214 m/sec). The Strouhal number is assumed to be 0.18 for a vortex shedding frequency. The smaller trip would, therefore, exhibit a flow-induced shedding frequency of

50.1 kHz in the boundary layer. This vortex shedding frequency is shown in figure 5 and lies in the damping region for a Mach 5.8 flow as computed by Arnal [11]. Thus, by generating a strong instability in this frequency region, the row of smaller trips act as a boundary layer stabilizer and delays the transition to turbulent flow as was seen in the heating rate data of figure 3. An extension of this technique for a practical, full scale, geometry might be to employ tandem rows of trips.

2) Passive Wavy Wall Trips

In another passive trip experiment, Fujii [14,15] has extended the tandem row of trips idea, by employing either a wavy wall or a sequential series of wires. Similar results are observed for each, but the wavy wall configuration will be considered here since it would appear to be the easiest to implement. The wavy wall consisted of 5 individual grooves located approximately 200 mm from the apex of a 5-degree half-angle cone model. Each groove has a trapezoidal cross-section of height 0.5 mm and the spacing between the grooves is 2 mm. The wavy-wall thus exhibits a cross between surface trips and surface cavities. The experiments were conducted in a pebble heated blowdown facility at Mach 7.1. Transition was detected by measuring heat transfer distributions using infrared (IR) thermography. Figure 6 shows the result of an experiment at 1000 K and 6 MPa {Figure 8(c) in Fujii [14, 15]}, in which the wavy configuration, with only 5 grooves, has a weak, but discernible effect in delaying transition.

Comparison of these results on a cone with the planar computations of Arnal [11] requires that they be made for the same Reynolds number based on the thickness of the boundary layer. Battin and Lin [16]. As a first step in the comparison, figure 7 shows a planar equivalent to the cone experiment with estimated flow patterns interacting with a trip/cavity configuration. The figure also illustrates the significant height of the trips relative to the boundary layer thickness, δ_p, a counter-intuitive development to traditional concepts using thin surface modifications. The interaction of the flow with the wavy wall (trip/cavity) configuration leads to the definition of a corrugation frequency, f_c, given by

$$f_c = u / s \qquad (2)$$

where the velocity, u, is effectively determined at the top of the grooves within the boundary layer (not the edge velocity), and, s, is the spacing of the peaks in the corrugation. For the 6 MPa experiment, u = 345 m/sec. Using this velocity and the separation of 2mm, results in a corrugation frequency, f_c = 173 kHz.

The second step in comparing with the planar calculations of Arnal [11] is to determine R_{δ^*} for use in the Mach 7 amplification rate curve. For this purpose, it is necessary to employ the cone-to-planar transition Reynolds number ratio, R_c / R_p . Although this ratio has been determined originally from purely geometric considerations, experiments have shown that the ratio is a function of the facility size and on the unit Reynolds number. It is speculated that facility noise, originating on the turbulent walls of a particular facility, is the major cause of this effect. Pate [17] has evaluated the ratio for a number of facilities and has found that it decreases from 2.2

to 1 over the Mach number range from 3 to 8. For the Fujii experiment at Mach 7.1, this ratio is 1.23. Figure 8 shows the amplification rate for the delay of transition observations shown in figure 6 using the Mach 7 computations of Arnal [11] at $R_{\delta^*} = 0.94 \times 10^4$. The wavy wall corrugation frequency, $f_c = 173$ kHz, is also shown in figure 8 and lies in the damping region of the amplification rate curve. The generation of a strong disturbance by the wavy wall in the damping region results in stabilization of the boundary layer flow and a delay of transition.

The reliance on a significant empirical factor depending on facility size for the cone to planar comparison is necessary, but unsettling. The implication of flow contamination from facility walls is similar to the mode 2 facility dependence mentioned earlier. These facility effects lead to many uncontrollable factors which hinder progress in fluid flow research and point to the need for improved ground based flow facilities.

3) Leading-Edge Bluntness

A "Reversal of Transition" was observed by Lysenko [18] with increasing leading-edge bluntness on a slender, insulated, flat-plate model at Mach 4. The model consisted of a polished steel flat plate 450 mm long with a bevel angle of the leading edge of 20 degrees. A sharp leading-edge of 0.02 mm bluntness was used as a baseline and is taken to be a direct measurement of the amplification rate for this condition. The bluntness, b, was then varied thru seven steps with the following values: 0.1, 1, 1.5, 2, 3, 5 and 10 mm. Measurements of transition were made using hot-wires and pressure gauges. Figure 9, {figure 13 in Lysenko}, shows an initial advance of transition with increasing bluntness Reynolds number and then a delay of transition as the bluntness is increased further. The seven numbers along the x-axis in figure 9 have been added here to denote the increasing values of bluntness.

Figure 10, {figure 12 in Lysenko}, shows experimental measurements of amplification rate for the baseline sharp leading-edge and two values of bluntness, 3 mm and 5 mm. This is one of the few experiments that have made measurements of amplification rate in the damping region. The dimensionless frequency parameter, F, employed by Lysenko, is converted to dimensional frequency, f, using the equation, [$f = (1/2\pi)\, R_0\, V\, F$], where R_0 is the associated Unit Reynolds number and V is the velocity incident on the leading-edge. Measured data points from Lysenko are left off in figure 10 for clarity.

Vortex shedding generated by the leading edge is assumed to account for the bluntness spectra. Using a Strouhal number of 0.18, the 5 mm bluntness and its measured peak frequency at 8 kHz predict an incident velocity on the edge of 222 m/sec. Likewise, the 3 mm bluntness and its measured peak frequency at 15 kHz would predict an incident velocity of 250 m/sec. Although there have not been any measurements of velocity in the detached shock region, these two velocities are within the range of the subsonic velocities to be expected between the sonic lines for this Mach number. The numbers, (5) and (6), along the x-axis and the vertical dotted lines in figure 10 show the location of the vortex shedding frequencies for the associated values of Strouhal number, bluntness, and velocity which are consistent with the peak frequencies measured experimentally. Based on this analysis, the vortex shedding

frequencies due to the blunt edges lie in the damping region defined by the baseline spectrum. The measured amplification rates for the 3 mm and 5 mm bluntness's also extend into the damping region for an appreciable range of dimensional frequency. This extension into the damping region parallels the observations of Lysenko and Maslow [19] in which it is possible to achieve complete stabilization of the flow with the aid of cooling (i.e. the boundary layer will only contain damped disturbances and laminar flow is extended). In summary, vortex shedding generated by a blunt leading-edge would be expected to stabilize the boundary layer and bring about a delay in transition from laminar to turbulent flow.

4) Active Spark Discharge

Using a spark discharge, Klein [20] has demonstrated the equivalence of high repetition rate discharges and physical trips to influence flow control. Three flat-plate models were used:

1) No protuberances on the surface,

2) A Row of Spheres 2.22 cm from the leading edge,

3) A Single Spark Discharge 2.22 cm from the leading edge.

On each model, skin friction measurements were made 14.92 cm downstream of the leading-edge. The spark discharge was run at several set frequencies between 1 and 32 kHz. Each model was tested at Mach numbers 1.98, 2.56, 3.53, and 3.88 over a range of free-stream Reynolds numbers. Figure 11 shows the size of the spheres (model 2) relative to the boundary layer thickness for the Mach 3.53 case. Figure 11 also includes an estimated height for the discharges (model 3), inferred from a localized microwave surface plasma generated by the author in a static laboratory experiment. Figure 12 {figure 6(c) in Klein} shows the increase in the skin-friction coefficient at Mach 3.53 as the frequency of the discharge is increased. The figure demonstrates the equivalence of high repetition rate discharges with physical trips (row of spheres). The discharge measurements shown represent a matrix of 5 of the frequencies employed and 9 values of the Reynolds number. The results for only a single spark discharge (model 3) lie in-between the no disturbance condition (model 1) and the level attained by the row of 0.8 mm spheres (model 2). The model 2 results agree with the calculated fully turbulent level. All of the frequencies employed in the laminar or transition region at Mach 3.53 resulted in an advance of transition. Figure 13 shows the amplification rate spectrum for four of these Reynolds numbers along with the positions of the discharge frequencies. All of the frequencies are in the amplification range for their respective Reynolds number, except for 32 kHz at 5.5 x 10^4 cm^{-1} and 6.6 x 10^4 cm^{-1}, which lie in the damping region. Data points for these two conditions were not reported {figure 6(c) in Klein [20]}.

At Mach 2.53, however, Klein indicated, in a brief quote, a reduction of skin-friction coefficients using high repetition rate discharges of 6 and 32 kHz {figure 6(b) in Klein [20]}:

> *"At Mach 2.53, it was observed that high frequency spark discharges were able to reduce skin-friction coefficients somewhat at unit Reynolds numbers at which normally turbulent boundary layers resulted at the measuring station."*

This observation of a reduction in skin-friction was not made in a laminar or transitional flow, but in a region where the flow had already transitioned to turbulence. In an established turbulent flow, the effect of higher frequencies to modify the flow is expected to be a subtle one. Figure 14 shows the amplification rate spectrum at $R_o = 1.56 \times 10^5$ cm^{-1} for Mach 2.56 (interpolation between Mach 2.2 and Mach 3 from Arnal [11]). In support of the observation of the reduction in skin-friction, the discharge frequencies shown in figure 14 are located both below (6 kHz) and above (32 kHz) the unstable portion of the amplification rate spectrum.

The main conclusion to be realized from the Klein experiments is the importance of the frequency (repetition rate) of forced plasma disturbances as an active influence on boundary layer flow control.

Recommendations for Future Research:

Development of forced damping using passive and active stabilizers in the boundary layer should be conducted in subsonic, supersonic and hypersonic ranges, for fuel efficiency, increased flow control, and increased range, respectively. In each of the three regimes, there will be a need to evaluate the various stabilizer frequencies and strengths. For this measure, the height and shape of the stabilizer relative to the boundary-layer thickness and the velocity distribution within the boundary-layer will be required.

The extension of the wavy-wall configuration to the subsonic range, in particular, may have the largest payoff thru increased fuel savings for commercial aircraft. The delay of transition using a wavy-wall by Fujii [14, 15] was achieved using only 5 grooves and a fixed separation of corrugation. In the extended wind tunnel effort, the number of grooves should be increased to strengthen and firmly establish the corrugation frequency. Ultimately, the grooves should cover the surface. Another interesting variation to the wavy-wall configuration would be to increase the separation of the peaks gradually in the downstream direction, hence allowing for a change in the Reynolds number. This procedure may allow the transition point to be delayed even further, perhaps indefinitely. The experiments should also be conducted on a flat-plate model, allowing a better correlation with theoretical calculations. As a starting point, the flat-plate stability diagram given by Cebeci and Cousteix [12] for Mach 0.90 is shown in figure 15. This Mach number approximates the cruising speed, Mach 0.85, of a commercial airliner. Two Reynolds numbers are selected; $R_{\delta^*} = 1.5 \times 10^3$ for wind tunnel tests, and $R_{\delta^*} = 5.5 \times 10^3$ for a closer simulation to flight. The amplification rate spectra for these two conditions are shown in figure 16. For the wind tunnel tests, a corrugation frequency of 2.4 kHz, as shown, would create disturbances in the damping region on the low frequency side of the amplification rate

spectrum. This same corrugation frequency would create disturbances in the damping region for the flight Reynolds number, but on the higher frequency side of the amplification rate curve.

Active, plasma, stabilizers should also be explored further since they may provide an alternative, or supplement, to passive stabilizers. Plasma stabilizers can operate at any desired frequency, offer no drag to the flow, and may offer the ultimate in (programmable) boundary layer flow control. Only a single active, plasma trip was employed by Klein [20]. Experiments with multiple plasma trips, including the use of parasitic trips, should be explored in order to increase their effectiveness. Active plasma trips (stabilizers) may be energetically prohibitive for application to a large surface area, but may be especially useful in smaller, more difficult to access flow regions.

All of the stabilizers discussed in this report, both passive and active, employed models having a simple geometry. Ultimate application to a flight configuration will have to confront many different configurations and flow environments.

Summary and Conclusions:

1) In the past, most experiments have shown that almost any physical perturbation in the boundary layer results in an advance of transition, but a few rare experiments have exhibited a delay of transition.
2) The height of the physical trips in both the Holloway and Sterrett [13] and Fujii [14, 15] experiments are a significant fraction of the boundary layer thickness. This observation is counter-intuitive to many of the earlier attempts to delay transition through thin surface modifications.
3) The frequency (repetition rate) of the induced disturbance is a key factor in the delay of transition and is dependent on the geometry of the trip (stabilizer) and the velocity that it encounters in the boundary layer.
4) The generation of strong disturbances in a laminar boundary-layer with a frequency (repetition rate) in the damping region of the associated amplification rate curve stabilizes the flow and delays transition.
5) An alternative to (passive) physical stabilizers would be (active) plasma stabilizers. These stabilizers can operate at any desired frequency, offer no drag to the flow, and may offer the ultimate in (programmable) boundary layer flow control.
6) It is anticipated that passive or active perturbations generated on the surface of the model will remain in the boundary layer for an appreciable distance downstream. This will be important in promulgating the delay effect downstream and the development of flow control techniques.

References:

[1] E. Reshotko, "Boundary-Layer Stability and Transition", Ann. Rev. Fluid Mech. **8,** 311-349 (1976).

[2] W. S. Saric, H. L. Reed, and E. J. Kerschen, "Boundary-Layer Receptivity to Freestream Disturbances", Ann. Rev. Fluid Mech. **34**, 291-319 (2002).

[3] M. J. Walsh, "Riblets", *AIAA Progress in Aeronautics and Astronautics: Viscous Drag Reduction in Boundary Layers,* edited by D. M. Bushnell and J. N. Hefner, Vol. 123, pp. 203-261 (1990).

[4] J. L. Potter, "Review of the Influence of Cooled Walls on Boundary-Layer Transition", AIAA J. **18** (8) 1010-1012 (1980).

[5] W. S. Saric, R. B. Carrillo, Jr., and M. S. Reibert, "Leading Edge Roughness as a Transition Control Mechanism", AIAA 98-0781 (1998).

[6] P. F. Brinich and N. Sands, "Effect of Bluntness on Transition for a Cone and a Hollow Cylinder at Mach 3.1", NACA TN-3979 (1957).

[7] J. L. Potter and J. D. Whitfield, "Effects of Slight Nose Bluntness and Roughness on Boundary-Layer Transition in Supersonic Flows", J. Fluid Mech. **12**, 501-535 (1962).

[8] T. C. Corke, M. L. Post, and D. M. Orlov, "Single Dielectric Barrier Discharge Plasma Enhanced Aerodynamics: Physics, Modeling and Applications", Exp. Fluids **46**, 1-26 (2009).

[9] J. H. M. Fransson, A. Talamelli, L. Brandt, and C. Cossu, "Delaying Transition to Turbulence by a Passive Mechanism", Phys. Rev. Letts. **96**, 064501 (2006).

[10] L. Mack "Linear Stability Theory and the Problem of Supersonic and Hypersonic Boundary-Layer Transition", AIAA J. **13** (3) 278-289 (1975).

[11] D. Arnal, "Laminar-Turbulent Transition Problems in Supersonic and Hypersonic Flows", In *Special Course on Aerothermodynamics of Hypersonic Vehicles*. AGARD-R-761, (1989).

[12] T. Cebeci and J. Cousteix, "*Modeling and Computation of Boundary-Layer flows",* Second Edition (2005), Horizons Publishing Inc., Long Beach.

[13] P. F. Holloway and J. R. Sterrett, "Effect of Controlled Surface Roughness on Boundary-Layer Transition and Heat Transfer at Mach Numbers of 4.8 and 6.0," NASA TN D-2054, (1964).

[14] K. Fujii, "Experiment of the Two-dimensional Roughness Effect on Hypersonic Boundary-Layer Transition," J. Spacecraft and Rockets **43**, 731 (2006).

[15] K. Fujii, "An Experiment of Two Dimensional Roughness Effect on Hypersonic Boundary-Layer Transition," AIAA Paper No. 2005-891, (2005).

[16] R. H. Battin and C. C. Lin, "On the Stability of the Boundary Layer over a Cone", J. Aeronautical Sciences **17**, 453-454 (1950).

[17] S. R. Pate, "Effects of Wind Tunnel Disturbances on Boundary-Layer Transition with Emphasis on Radiated Noise: A Review", AIAA 80-0431 (1980).

[18] V. L. Lysenko, "High-Speed Boundary-Layer Stability and Transition," Int. J. Mech. Sci. **35**, 921 (1993).

[19] V. L. Lysenko and A. A. Maslov, "The Effect of Cooling on Supersonic Boundary-Layer Stability", J. Fluid Mech. **147**, 39-52 (1984).

[20] E. J. Klein, "Excitation of Boundary-Layer Turbulence Through Spark Discharges," NASA TN D-6378, (1971).

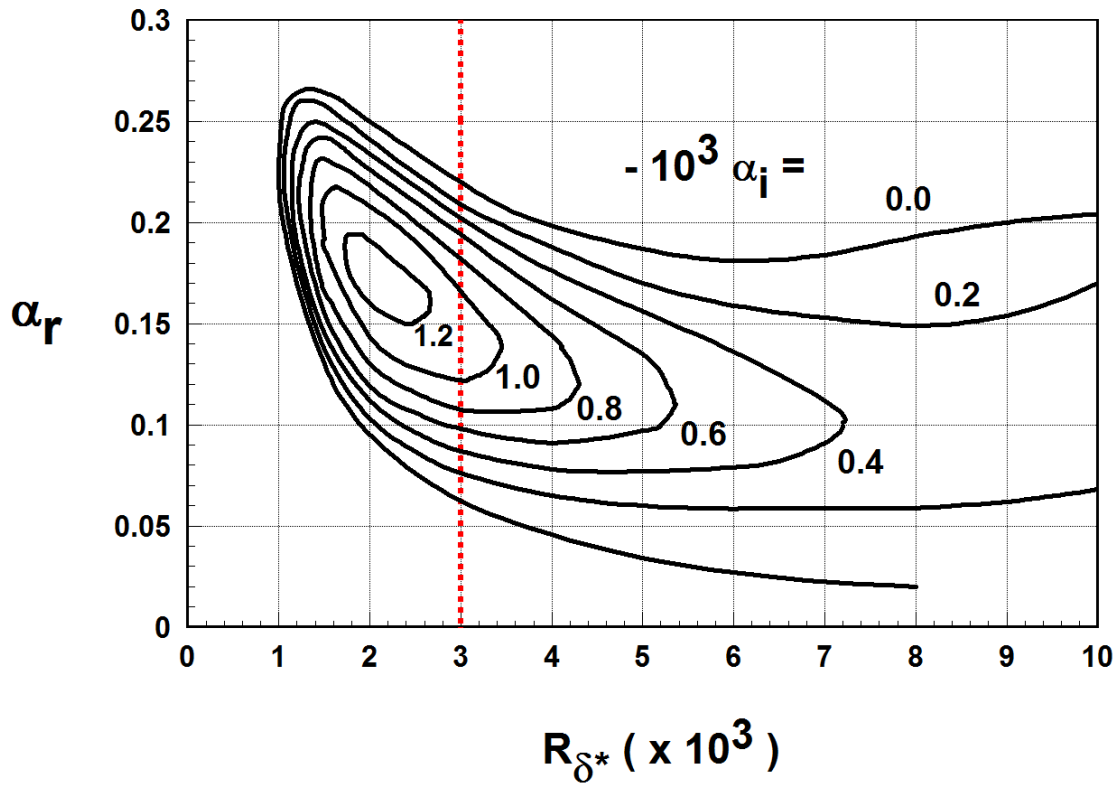

Figure 1: Stability Diagram for Mach 2.2, Arnal [11].

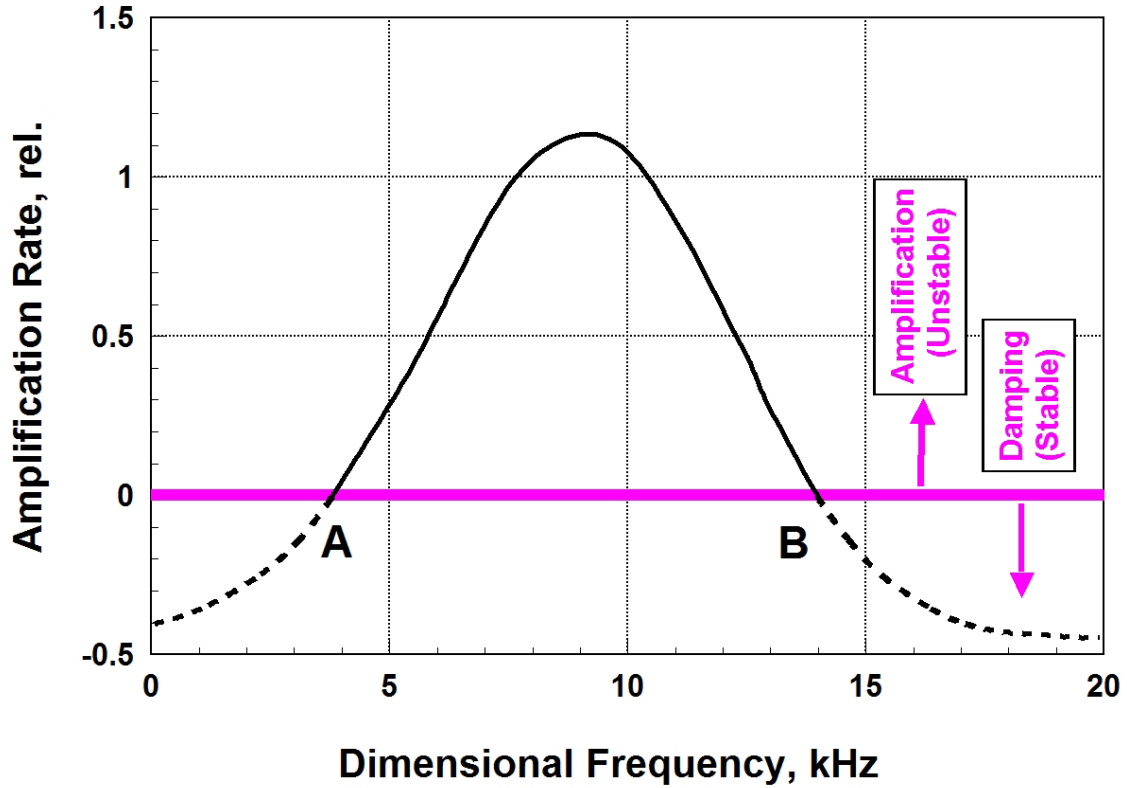

Figure 2: Amplification Rate vs. Dimensional Frequency for Mach 2.2 and $R_{\delta^*} = 3 \times 10^3$

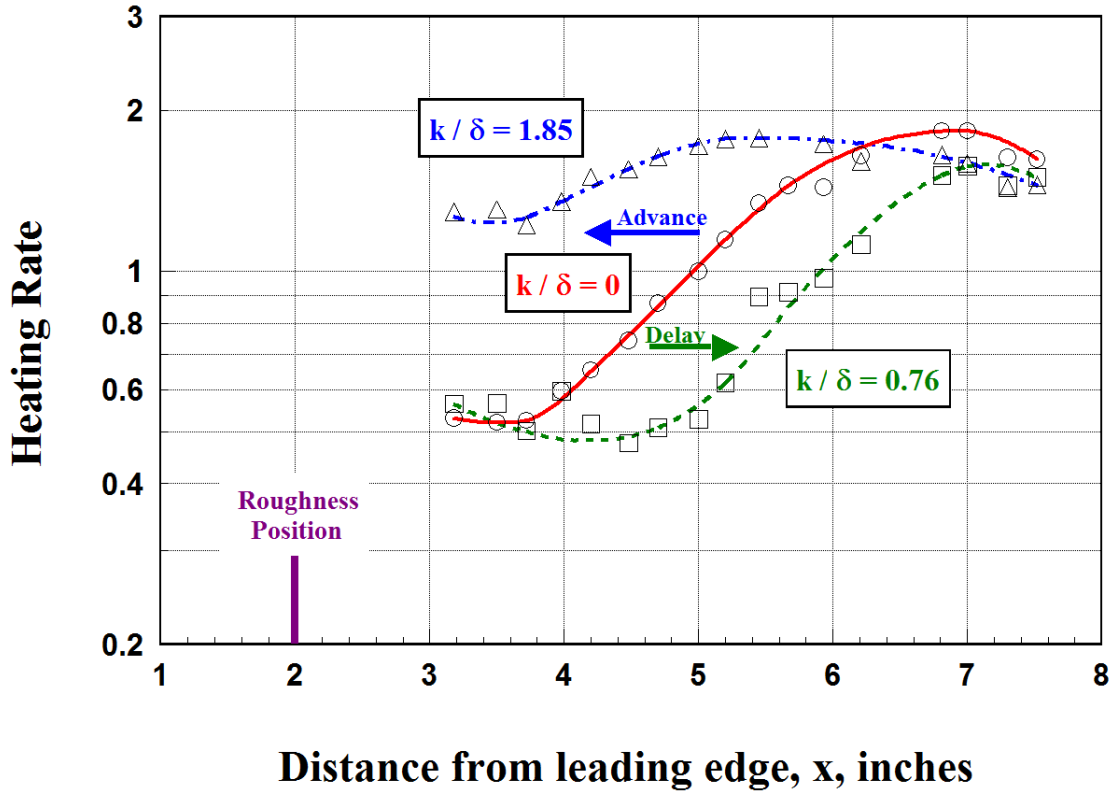

Figure 3: Delay and Advance of Transition at Mach 6 [13].

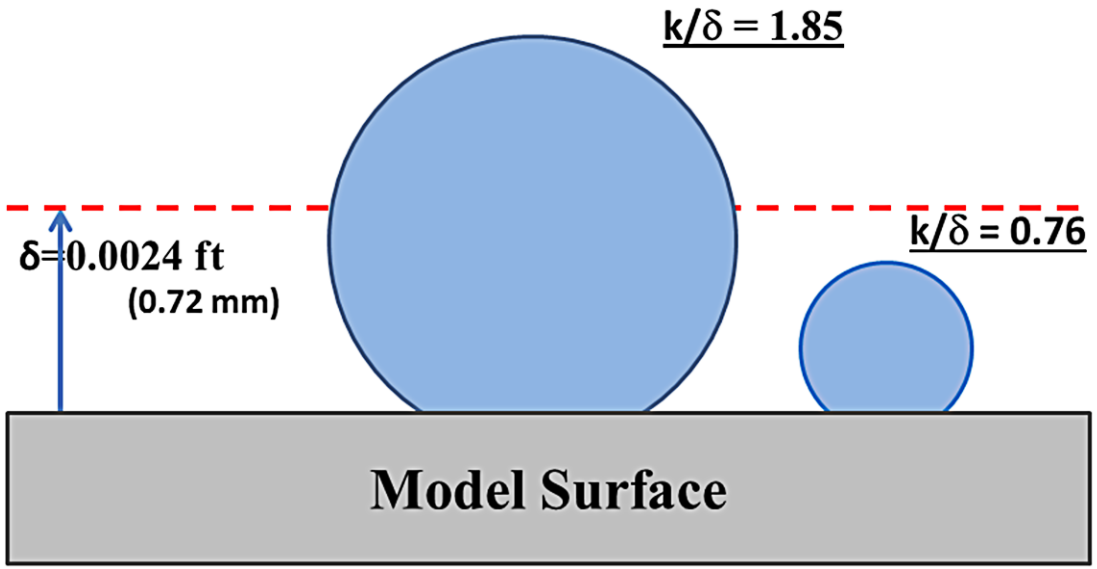

Figure 4: Dimensions for the Two Trips Described in Figure 3.

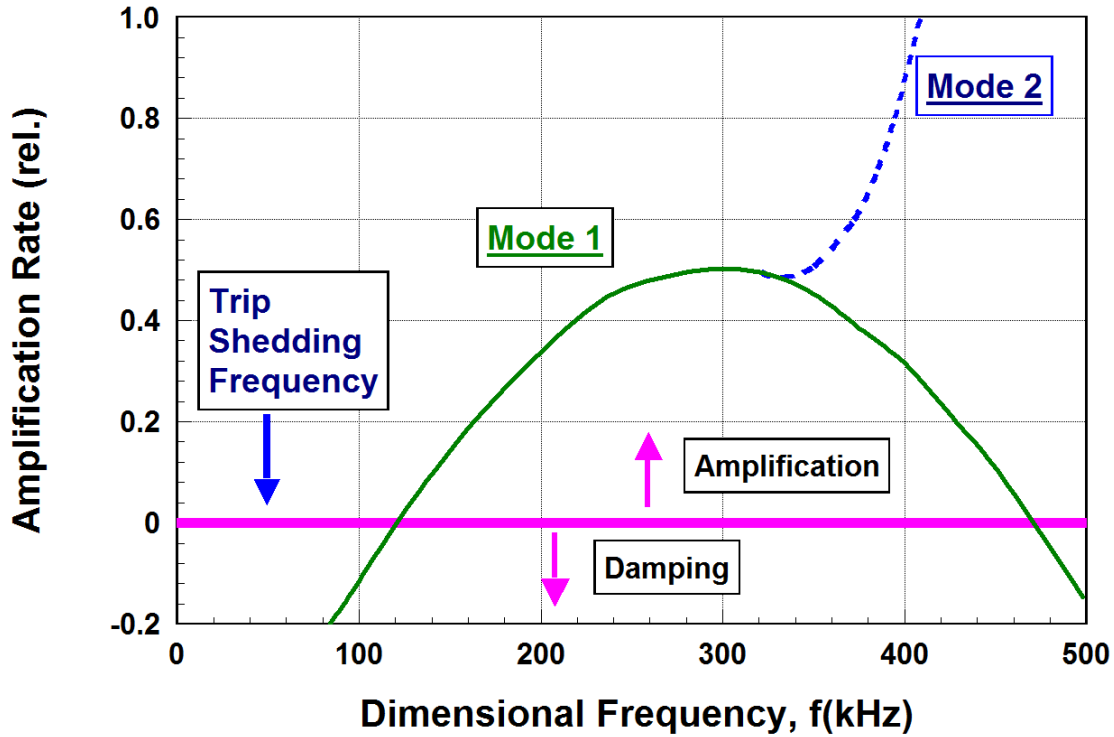

Figure 5: Vortex Shedding Frequency Relative to the Amplification Rate Spectrum at Mach 5.8 (Approximation to Mach 6).

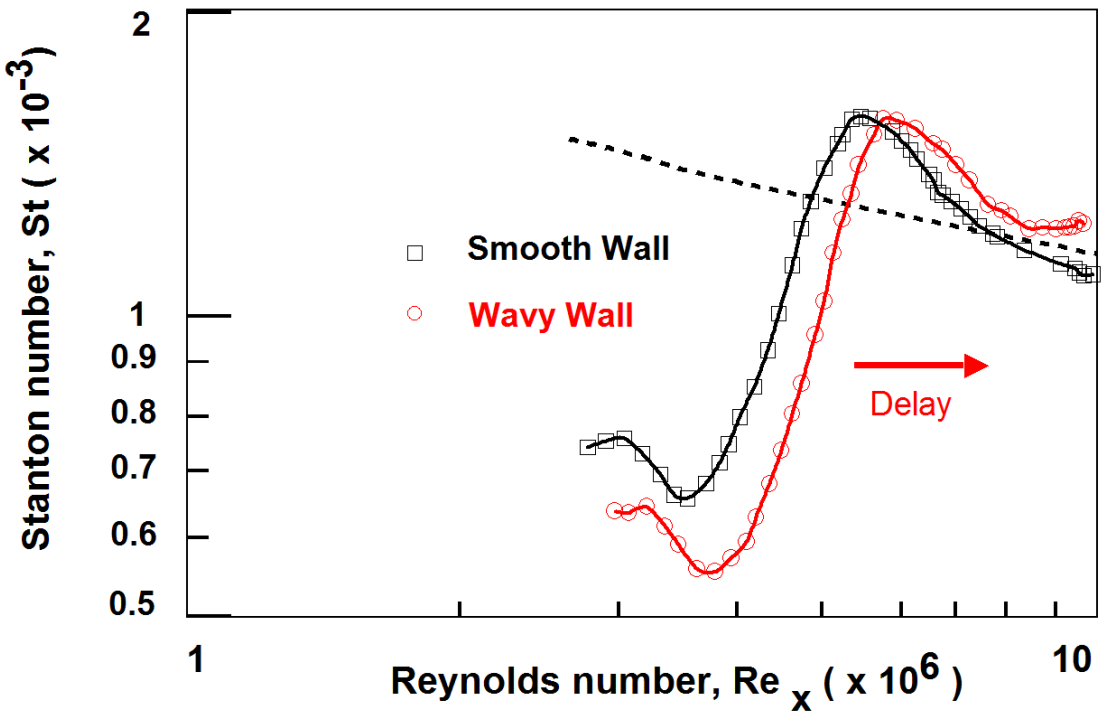

Figure 6: Delay of Transition using a Wavy Wall at Mach 7.1, Fujii [14, 15].

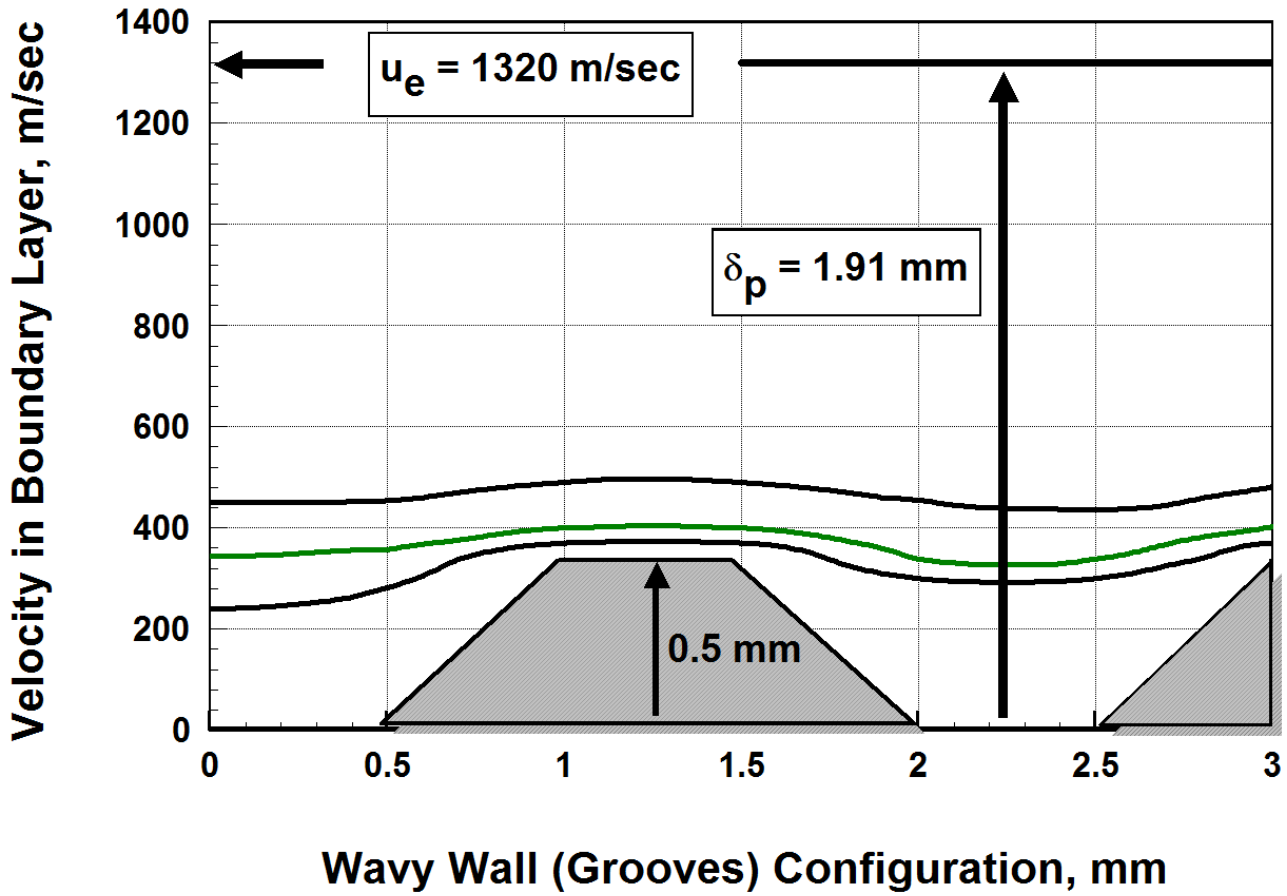

Figure 7: Planar Equivalent of Cone Boundary Layer at Mach 7.1

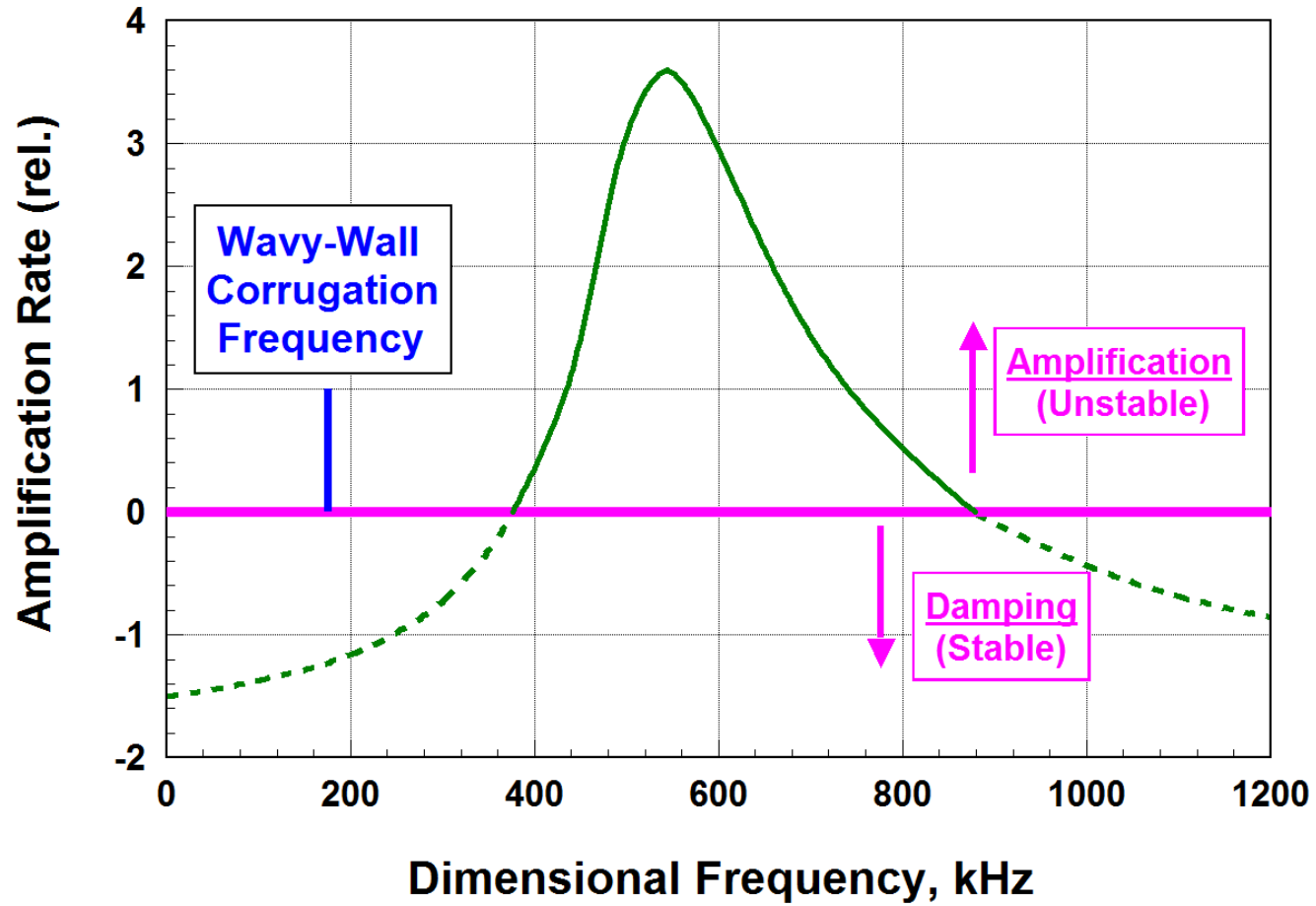

Figure 8: Amplification Rate Spectrum for Mach 7 [11]. The Wavy Wall Corrugation Frequency [f_C = 173 kHz] lies in the Damping Region.

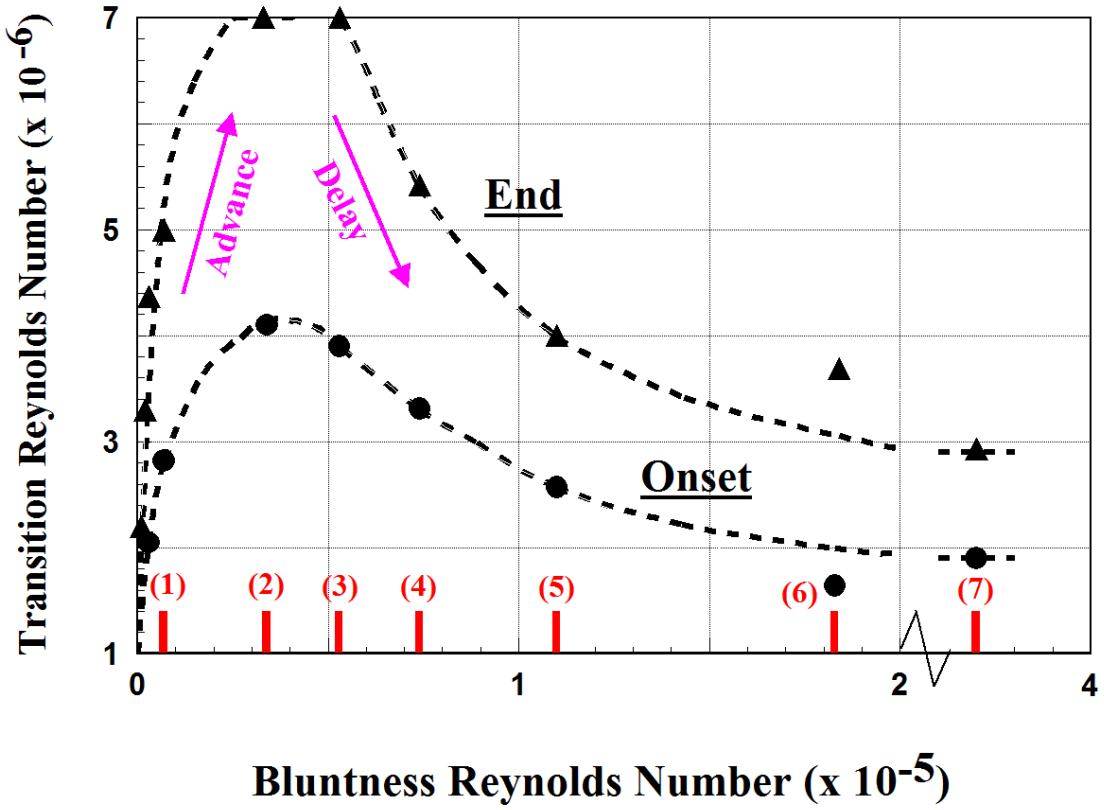

Figure 9: "Reversal of Transition" as observed by Lysenko [18] at Mach 4.

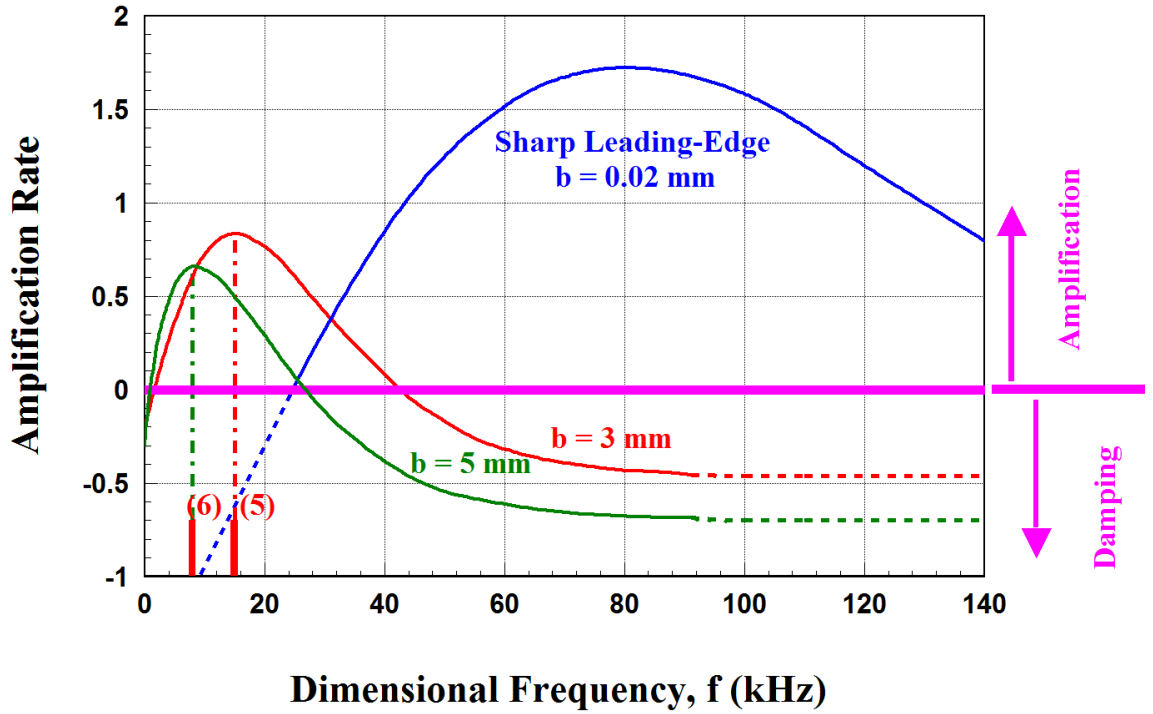

Figure 10: Measurement of Amplification Rates by Lysenko [18].

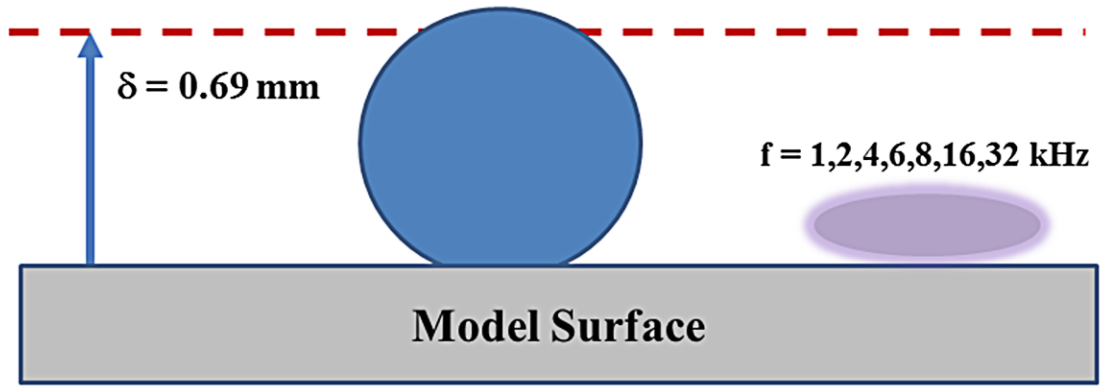

Figure 11: Sphere Size Relative to Boundary Layer Thickness at Mach 3.53, Klein [20]. An Estimate for the Size of the Surface Discharges is also shown.

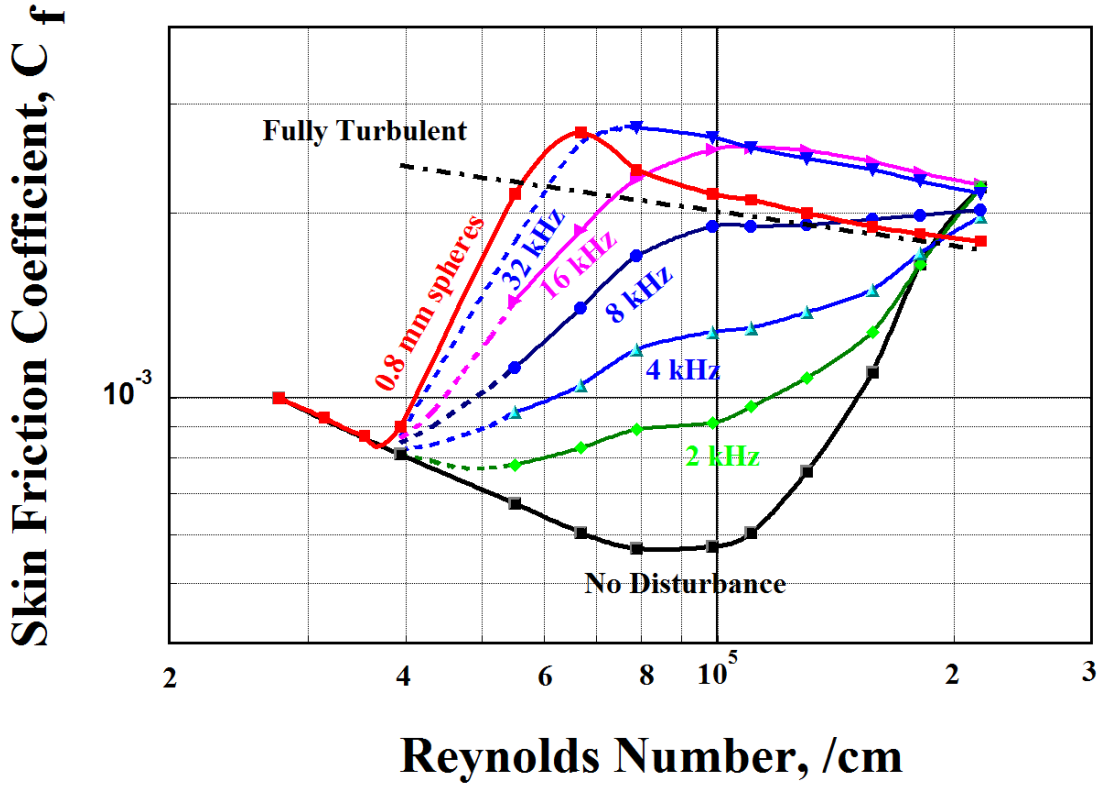

Figure 12: Increase in Skin Friction Coefficient at Mach 3.53 with Increasing Discharge Frequency, Klein [20].

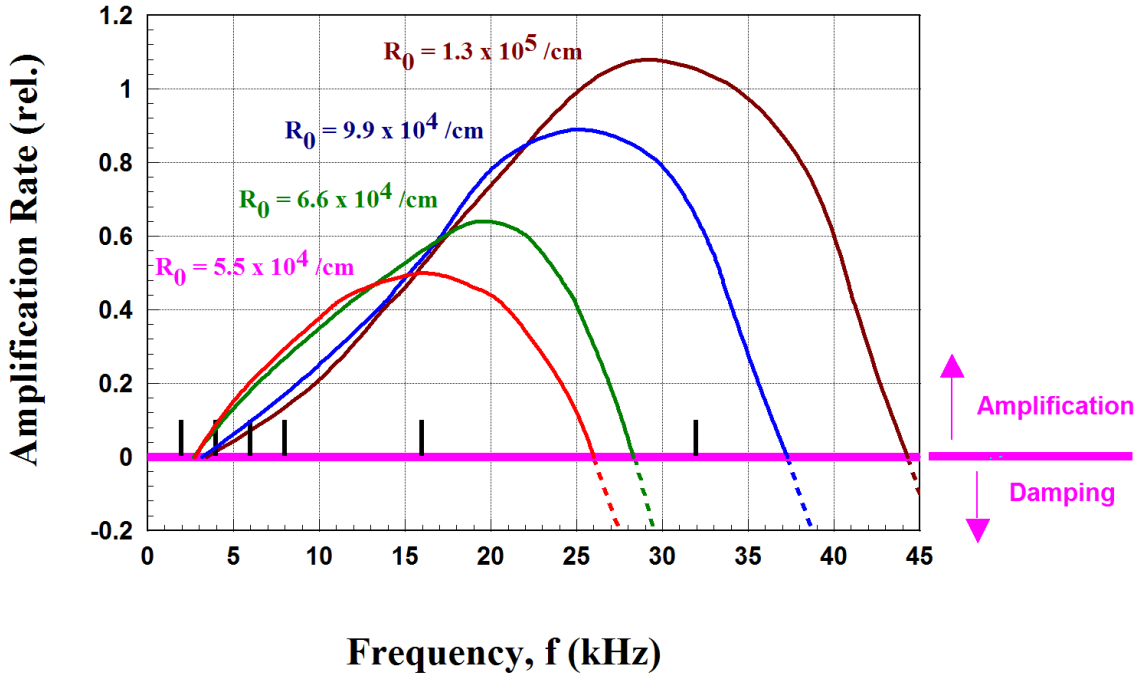

Figure 13: Amplification Rate Spectrum for Specific Reynolds Numbers at Mach 3.53, Klein [20].

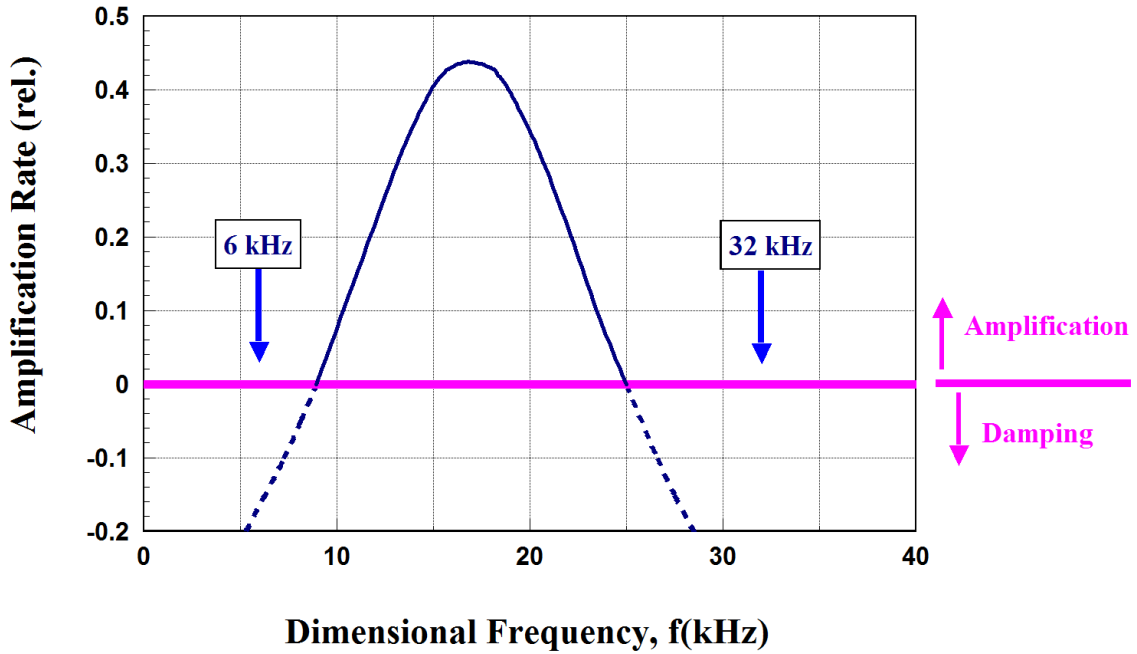

Figure 14: Amplification Rate Spectrum for $R_o = 1.56 \times 10^5$ cm^{-1} and Mach 2.56. Mach 2.56 Interpolated between Mach 2.2 and Mach 3, Arnal [11].

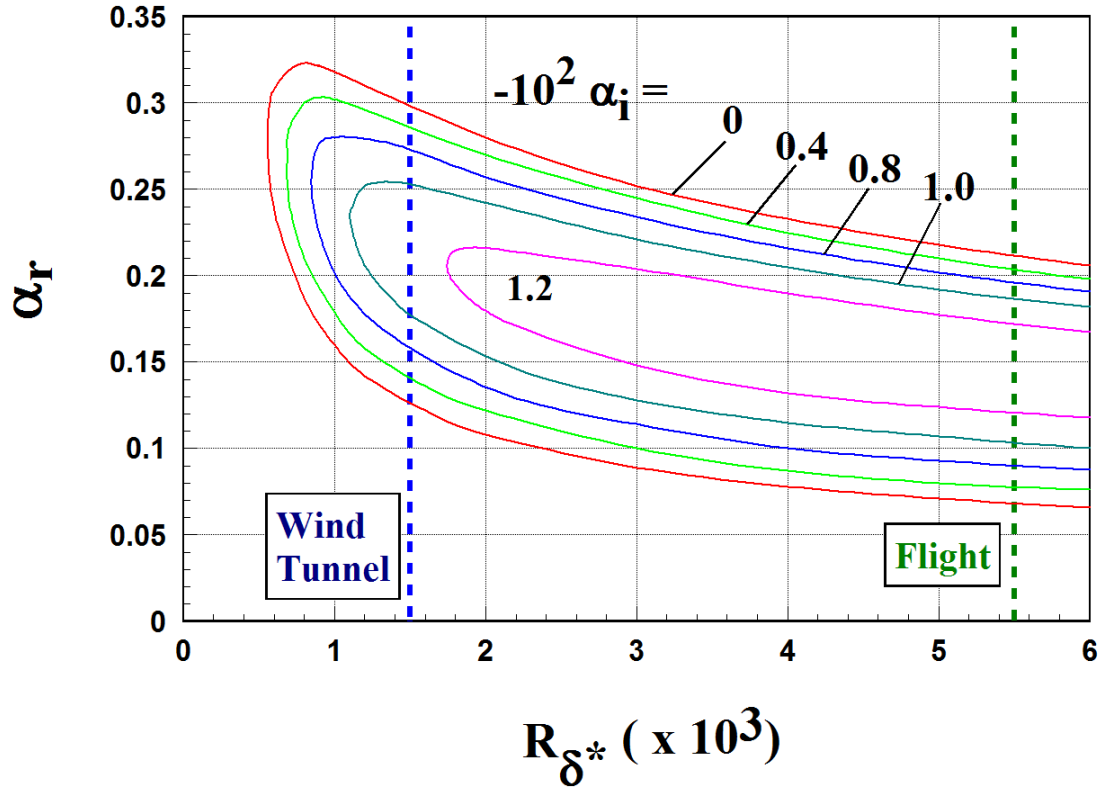

Figure 15: Stability Diagram for Mach 0.9, Cebeci and Cousteix [12].

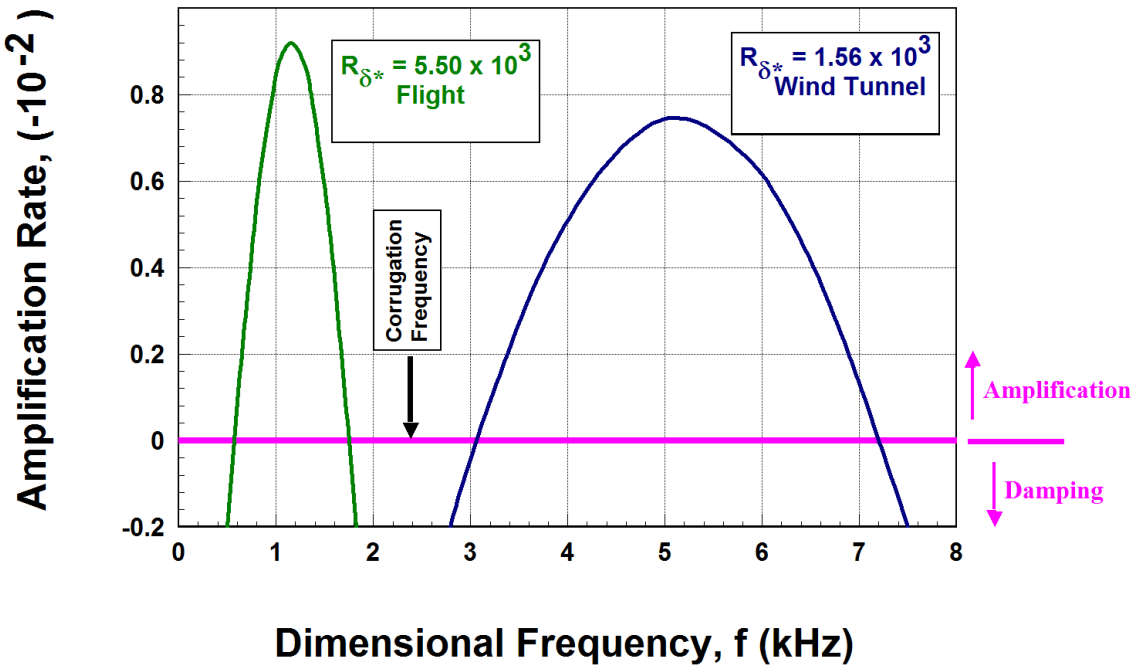

Figure 16: Amplification Rate Spectrum for Mach 0.9 and Two Selected Reynolds numbers.

REPORT DOCUMENTATION PAGE

Form Approved
OMB No. 0704-0188

1. REPORT DATE *(DD-MM-YYYY)*	2. REPORT TYPE	3. DATES COVERED *(From - To)*
01- 11 - 2014	Technical Memorandum	

4. TITLE AND SUBTITLE

Delay of Transition Using Forced Damping

5a. CONTRACT NUMBER

5b. GRANT NUMBER

5c. PROGRAM ELEMENT NUMBER

6. AUTHOR(S)

Exton, Reginald J.

5d. PROJECT NUMBER

5e. TASK NUMBER

5f. WORK UNIT NUMBER

305295.01.40.07

7. PERFORMING ORGANIZATION NAME(S) AND ADDRESS(ES)

NASA Langley Research Center
Hampton, VA 23681-2199

8. PERFORMING ORGANIZATION REPORT NUMBER

L-20496

9. SPONSORING/MONITORING AGENCY NAME(S) AND ADDRESS(ES)

National Aeronautics and Space Administration
Washington, DC 20546-0001

10. SPONSOR/MONITOR'S ACRONYM(S)

NASA

11. SPONSOR/MONITOR'S REPORT NUMBER(S)

NASA/TM-2014-218551

12. DISTRIBUTION/AVAILABILITY STATEMENT

Unclassified - Unlimited
Subject Category 02
Availability: NASA CASI (443) 757-5802

13. SUPPLEMENTARY NOTES

14. ABSTRACT

Several experiments which have reported a delay of transition are analyzed in terms of the frequencies of the induced disturbances generated by different flow control elements. Two of the experiments employed passive stabilizers in the boundary layer, one leading-edge bluntness, and one employed an active spark discharge in the boundary layer. It is found that the frequencies generated by the various elements lie in the damping region of the associated stability curve. It is concluded that the creation of strong disturbances in the damping region stabilizes the boundary-layer and delays the transition from laminar to turbulent flow.

15. SUBJECT TERMS

Delay of Transition; Flow Control; Forced Damping; Turbulent Flow

16. SECURITY CLASSIFICATION OF:			17. LIMITATION OF ABSTRACT	18. NUMBER OF PAGES	19a. NAME OF RESPONSIBLE PERSON
a. REPORT	b. ABSTRACT	c. THIS PAGE			STI Help Desk (email: help@sti.nasa.gov)
					19b. TELEPHONE NUMBER *(Include area code)*
U	U	U	UU	32	(443) 757-5802